CHEMISTRY
A EUROPEAN JOURNAL

FULL PAPER

DOI: 10.1002/chem.201204391

Terminal and Bridging Parent Amido 1,5-Cyclooctadiene Complexes of Rhodium and Iridium

Inmaculada Mena,[a] E. A. Jaseer,[b] Miguel A. Casado,*[a] Pilar García-Orduña,[a] Fernando J. Lahoz,[a] and Luis A. Oro*[a, b]

Abstract: The ready availability of rare parent amido d^8 complexes of the type $[\{M(\mu\text{-}NH_2)(cod)\}_2]$ (M = Rh (**1**), Ir (**2**); cod = 1,5-cyclooctadiene) through the direct use of gaseous ammonia has allowed the study of their reactivity. Both complexes **1** and **2** exchanged the di-olefines by carbon monoxide to give the dinuclear tetracarbonyl derivatives $[\{M(\mu\text{-}NH_2)(CO)_2\}_2]$ (M = Rh or Ir). The diiridium(I) complex **2** reacted with chloroalkanes such as CH_2Cl_2 or $CHCl_3$, giving the diiridium(II) products $[(Cl)(cod)Ir(\mu\text{-}NH_2)_2Ir(cod)(R)]$ (R = CH_2Cl or $CHCl_2$) as a result of a two-center oxidative addition and concomitant metal–metal bond formation. However, reaction with $ClCH_2CH_2Cl$ afforded the symmetrical adduct $[\{Ir(\mu\text{-}NH_2)(Cl)(cod)\}_2]$ upon release of ethylene. We found that the rhodium complex **1** exchanged the di-olefines stepwise upon addition of selected phosphanes (PPh_3, $PMePh_2$, PMe_2Ph) without splitting of the amido bridges, allowing the detection of mixed COD/phosphane dinuclear complexes $[(cod)Rh(\mu\text{-}NH_2)_2Rh(PR_3)_2]$, and finally the isolation of the respective tetraphosphanes $[\{Rh(\mu\text{-}NH_2)(PR_3)_2\}_2]$. On the other hand, the iridium complex **2** reacted with PMe_2Ph by splitting the amido bridges and leading to the very rare terminal amido complex $[Ir(cod)(NH_2)(PMePh_2)_2]$. This compound was found to be very reactive towards traces of water, giving the more stable terminal hydroxo complex $[Ir(cod)(OH)(PMePh_2)_2]$. The heterocyclic carbene IPr (IPr = 1,3-bis(2,6-diisopropylphenyl)imidazol-2-ylidene) also split the amido bridges in complexes **1** and **2**, allowing in the case of iridium to characterize in situ the terminal amido complex $[Ir(cod)(IPr)(NH_2)]$. However, when rhodium was involved, the known hydroxo complex [Rh(cod)(IPr)(OH)] was isolated as final product. On the other hand, we tested complexes **1** and **2** as catalysts in the transfer hydrogenation of acetophenone with *i*PrOH without the use of any base or in the presence of Cs_2CO_3, finding that the iridium complex **2** is more active than the rhodium analogue **1**.

Keywords: cyclooctadienyl ligands · hydrogen transfer · iridium · parent amido · rhodium

Introduction

In general, the chemistry of amido late-metal complexes (M–NHR; R = alkyl, aryl) has experienced a substantial evolution during the two past decades, from which reliable methods of synthesis have been developed.[1] The main reason behind these efforts lies in the crucial participation of these species in relevant homogeneous catalytic processes such as hydroamination,[2] C–N coupling reactions,[3] and transfer hydrogenation to unsaturated substrates,[4] among other organic transformations.[5] However, related work on parent amido late-metal complexes (M–NH_2) has been far less developed, even though these complexes are thought to be intermediates in catalytic homogeneous transformations such as coupling between ammonia and aryl halides[6] or boronic acids[7] to give primary aryl amines. More importantly, an isolated terminal parent amido complex of palladium has been reported to undergo C–N reductive elimination to yield an aryl amine.[8]

The scarceness of methods to generate stable parent amido late-metal species may be considered a factor of relevance to explain the delayed study of the catalytic performance of parent amido late-metal complexes when compared with the related aryl- or alkyl amido species. As a matter of fact, it must be pointed out that these species are very rare and no general synthetic methods have been developed for their preparation.[9] So far, rational synthetic routes to these compounds involve mainly salt metathesis reactions that displace halogen ligands with amido nucleophiles,[10] dehydrohalogenation of NH_3 metallic adducts,[11] or deprotonation of cationic NH_3 adducts with strong bases.[12] Recently, parent-amido-bridged complexes of ruthenium and iridium

[a] Dipl.-Chem. I. Mena, Dr. M. A. Casado, Dr. P. García-Orduña, Prof. F. J. Lahoz, Prof. L. A. Oro
Instituto de Síntesis Química y Catálisis Homogénea ISQCH
Universidad de Zaragoza-CSIC
C/Pedro Cerbuna, 12, 50009 Zaragoza (Spain)
Fax: (+34) 976-761-187
E-mail: mcasado@unizar.es
oro@unizar.es

[b] Dr. E. A. Jaseer, Prof. L. A. Oro
Centre of Research Excellence in Petroleum and Petrochemicals
King Fahd University of Petroleum & Minerals
Dhahran 31261 (Saudi Arabia)

Supporting information for this article is available on the WWW under http://dx.doi.org/10.1002/chem.201204391.

have been obtained by transfer hydrogenation to dinuclear azido-bridged complexes with 2-propanol,[13] and a terminal amido iridium complex has been isolated from the hydrogenation of a unique Ir≡N nitrido compound.[14] It is important to mention that none of these synthetic methods makes use of ammonia as the source of "NH_2" fragments, which we believe is a crucial factor to achieve further functionalization of ammonia.[15]

In this line, there are some reports concerning the formation of amido complexes of Ir through oxidative addition processes to afford parent-amido-bridged or terminal species,[16] a phenomenon that was further confirmed by Hartwig et al., who reported on the formal oxidative addition of ammonia to an electronic-rich Ir^I pincer system, leading to the isolation of the first terminal amido hydrido Ir^{III} complex.[17] On the other hand, heterolytic splitting of ammonia was very recently achieved with iridium[18] and ruthenium[19] systems through metal–ligand cooperation. These methodologies lead to parent amido late-metal complexes by utilizing NH_3 as the direct source for the amido ligands, which we believe is the right approach to achieve further functionalization of ammonia. Accordingly to this statement, we have recently disclosed a novel strategy that allows the high-yield access to parent-amido-bridged complexes of Rh^I and Ir^I through heterolytic splitting of gaseous ammonia under very mild conditions.[20]

The ready availability of these unusual species through this protocol has allowed us to assess their reactivity towards a variety of substrates. So far, the reactivity of terminal parent amido complexes has been focused in proton exchange processes with weak acids,[11a, 12b, 21] insertions of carbon monoxide into the N–H bond,[10b] and reductive elimination of ammonia,[11b] a work that evidences a high basicity at the terminal amido nitrogen, which bears an exposed and reactive free electron pair. The situation is quite different in bridging parent amido complexes, in which the lone electronic pair is usually tightly bounded in a dative fashion to a second metal.[13,16a,b,f,18,24] In this context, a significant contribution has been recently reported dealing with the role of [Ir-NH_2-Ir] linkages in catalytic transfer hydrogenation, enlightening a novel binuclear, outer-sphere Noyori-like mechanism, in which the NH_2 groups behave as non-innocent ligands playing a key role in alcohol dehydrogenation and imido formation.[25]

Results and Discussion

In a preliminary communication we reported on the facile and high-yield access to Rh^I and Ir^I parent amido complexes directly with gaseous ammonia.[20] In this way, bubbling NH_3 to ethereal solutions of the methoxo-bridged complexes [{M(μ-OMe)(cod)}$_2$] (M = Rh, Ir; cod = 1,5-cyclooctadiene) at atmospheric pressure and low temperatures (−5 °C) afforded amido-bridged complexes of formulae [{M(μ-NH_2)(cod)}$_2$] (M = Rh (**1**), Ir (**2**)) in excellent yields (Scheme 1). Even though these reactions are reversible, the poor solubility of complexes **1** and **2** in diethyl ether allowed their easy isolation. Complexes **1** and **2** are quite sensitive towards moisture; as a matter of fact, addition of stoichiometric amounts of water to [D_6]benzene solutions of **1** and **2** afforded the known hydroxo-bridged complexes [{M(μ-OH)(cod)}$_2$] (M = Rh, Ir), upon release of ammonia, as confirmed by NMR measurements.

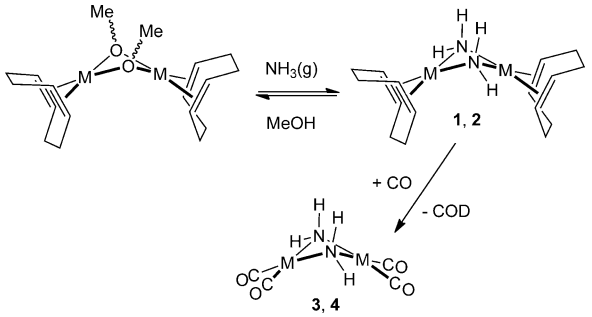

Scheme 1. Synthesis of [{M(μ-NH_2)(cod)}$_2$] (M = Rh (**1**), Ir (**2**)) and the tetracarbonyl derivatives [{M(μ-NH_2)(CO)$_2$}$_2$] (M = Rh (**3**), Ir (**4**)).

The structure of complex **1** has been recently reported.[20] In the present study, X-ray diffraction analysis of complex **2** confirms that both complexes exhibit similar structural features. The main difference between them concerns their asymmetric unit contents: two and three crystallographically independent but chemically identical molecules for complex **1** and **2**, respectively. Only one of those molecules of complex **2** is depicted in Figure 1, and selected bond lengths and angles are reported in Table 1. Both complexes are dinu-

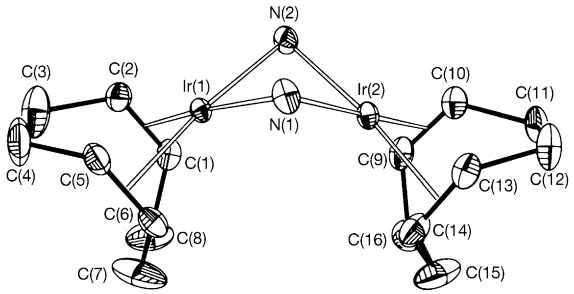

Figure 1. Molecular structure of complex **2**.

Table 1. Selected bond lengths [Å] and angles [°] for complex **2**.[a]

Ir(1)–N(1)	2.071(5)	Ir(2)–N(1)	2.075(5)
Ir(1)–N(2)	2.074(5)	Ir(2)–N(2)	2.081(5)
Ir(1)–M(1)	1.989(7)	Ir(2)–M(3)	1.996(6)
Ir(1)–M(2)	1.985(5)	Ir(2)–M(4)	1.993(7)
C(1)–C(2)	1.405(8)	C(9)–C(10)	1.386(9)
C(5)–C(6)	1.397(9)	C(13)–C(14)	1.377(10)
Ir(1)···Ir(2)	2.8146(3)		
N(1)-Ir(1)-N(2)	76.4(2)	N(1)-Ir(2)-N(2)	76.2(2)
N(1)-Ir(1)-M(1)	170.7(3)	N(1)-Ir(2)-M(3)	174.0(2)
N(1)-Ir(1)-M(2)	97.3(2)	N(1)-Ir(2)-M(4)	97.5(3)
N(2)-Ir(1)-M(1)	97.3(2)	N(2)-Ir(2)-M(3)	98.2(2)
N(2)-Ir(1)-M(2)	172.2(2)	N(2)-Ir(2)-M(4)	172.1(2)

[a] M(1), M(2), M(3), and M(4) represent the midpoints of the C(1)–C(2), C(5)–C(6), C(9)–C(10), and C(13)–C(14) bonds, respectively.

clear, formed by two "M(cod)" fragments bridged by two amido groups. The metal atoms exhibit a distorted square-planar coordination, involving two N atoms and the olefinic bonds to which they are bonded in a η^2-C=C fashion. An indication of the distortion from an ideal square-planar coordination in **2** comes from the fact that the iridium atoms lie 0.1081(3) and 0.0652(3) Å out of the least-square plane (formed by the two N atoms and the mid-points of the olefinic bonds) towards the other metal.

As in complex **1**, the four-membered ring "IrNIrN" of complex **2** shows a folded conformation; the dihedral angle between the coordination planes defined by N(1)-Ir(1)-N(2) and N(1)-Ir(2)-N(2) is 119.2(4)°, and consequently, a relatively short metal–metal distance of 2.8146(3) Å was observed. This value, shorter than that found in the related $[\{Ir(\mu\text{-}OEt)(cod)\}_2]$ complex, 2.8958(11) Å,[26] is close to the mean value found in dinuclear Ir compounds involving two bridging N atoms (2.584–2.968 Å, mean value 2.781(12) Å).[27] In fact a deeper analysis of these "IrNIrN" central cores revealed a direct relationship between the intermetallic distance and the four-membered-ring folding (similar to that observed for "RhORhO" fragments).[28] Values on the three independent molecules of compound **2** nicely follow the general trend (see the Supporting Information).

Complexes **1** and **2** exchanged the di-olefines upon exposure to carbon monoxide at atmospheric pressure, affording complexes $[\{M(\mu\text{-}NH_2)(CO)_2\}_2]$ (M = Rh (**3**), Ir (**4**)) as yellow solids in moderate yields (Scheme 1). Yellow single crystals of **4** were grown from a concentrated solution of the complex in $[D_6]$benzene at room temperature. The molecular structure of complex **4**, very similar to the precursor complex **2**, is depicted in Figure 2. Selected geometrical parameters are reported in Table 2. Complex **4** is a dinuclear Ir complex formed by two "$Ir(CO)_2$" fragments related by a crystallographic two-fold axis symmetrically bridged by two amido groups. The metal coordination is less deviated from an ideal square-planar geometry than in **2**, as it lies only 0.0401(2) Å out of plane. The dihedral angle between the NIrN planes (126.92(15)°) is slightly superior to that shown in **2**, therefore leading to a longer intermetallic distance of 2.9576(4) Å, which compares well with that shown by the related amido-bridged complex $[\{Ir(\mu\text{-}NH(p\text{-}C_6H_4CH_3))(CO)_2\}_2]$ (2.933(1) Å),[29] and follow the general trend previously commented.

The amido groups behave as strong hydrogen donors towards oxygen atoms of terminal carbonyls of adjacent molecules, forming hydrogen-bond rings $R_2^2(10)$ (Table 3 and Figure 3). Thus, hydrogen networks, along the *c* and *a*+*c* directions, are established at a supramolecular level in the crystalline structure of **4**.

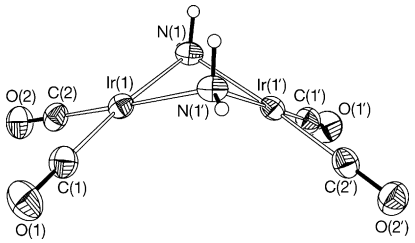

Figure 2. Molecular structure of complex **4**.

Table 2. Selected bond lengths [Å] and angles [°] for complex **4**.[a]

Ir(1)···Ir(2)	2.9577(4)	Ir(1)–N(1)	2.082(4)
Ir(1)–C(1)	1.859(6)	Ir(1)–C(2)	1.858(6)
N(1)-Ir(1)-N(1′)	75.0(2)	N(1′)-Ir(1)-C(1)	97.4(2)
N(1)-Ir(1)-C(1)	172.1(2)	N(1′)-Ir(1)-C(2)	172.4(2)
N(1)-Ir(1)-C(2)	97.7(2)	C(1)-Ir(1)-C(2)	89.8(2)

[a] Primed atoms are related to the non-primed ones by $-x$, y, $1/2-z$ symmetry operation.

Table 3. Bond lengths and angles for the hydrogen-bonding scheme in complex **4**.[a]

	D–H [Å]	H···A [Å]	D···A [Å]	D–H···A [°]
N(1)–H(2)···O(2″)	0.86(2)	2.52(5)	3.209(7)	137(2)
N(1)–H(2)···O(1^{iv})	0.86(4)	2.64(4)	3.325(5)	138(2)
N(1)–H(1)···O(2^{v})	0.87(7)	2.84(8)	3.274(7)	112(5)

[a] Symmetry operation ″) $-x$, $-y+1$, $-z$; iv) $x-1/2$, $1/2-y$, $z-1/2$; v) $-x$, $-y$, $-z$.

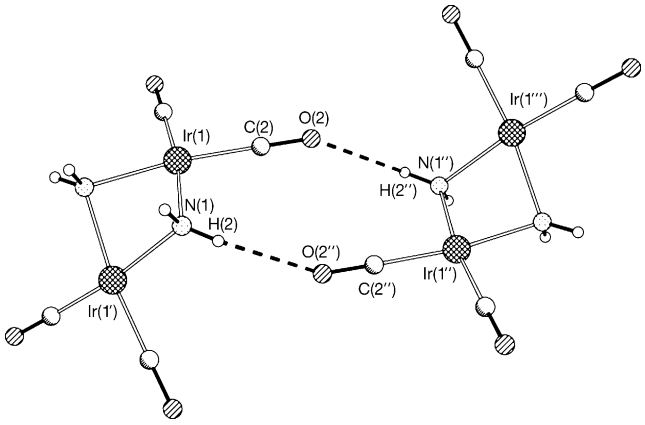

Figure 3. One of the hydrogen-bonded network established in solid structure of **4**. Symmetry operations: ′) $-x$, y, $1/2-z$, ″) $-x$, $1-y$,$-z$, ‴) x, $1-y$, $z-1/2$.

The ^{1}H NMR spectra of the carbonyl the complexes **3** and **4** were featureless, showing a lone broad signal ($\delta = -1.40$ and -0.25 ppm for complexes **3** and **4**, respectively) from the amido ligands at all temperatures in $[D_8]$toluene. These amido protons correlated to the nitrogen resonances giving signals at $\delta = -45.0$ and 5.1 ppm for **3** and **4**, respectively, as confirmed by ^{1}H–^{15}N HMBC measurements. The $^{13}C\{^1H\}$ NMR spectra were also very simple, because all the carbonyls were found to be chemically equivalent. However, IR data from solutions of complexes **3** and **4** in THF were more informative; both spectra displayed a set of three strong absorption bands for the terminal carbonyls, in agreement with the bent conformation of the molecular frame-

work with C_{2v} symmetry, as observed in the solid state for **4**. This structural information indicated that complexes **3** and **4** should be isostructural in solution. It is interesting to have a close look to the $\tilde{\nu}$(CO) stretching frequencies of complexes **3** ($\tilde{\nu}$ = 2079, 2042, 1970 cm^{-1}) and **4** ($\tilde{\nu}$ = 2059, 2035, 1972 cm^{-1}) and cross check them with those shown by structurally related open-book complexes of the type [{M(μ-L)$(CO)_2$}$_2$] (L = SR,[30] OR,[31] NHR[32]). The comparison clearly shows that the tetracarbonyl parent amido complexes **3** and **4** display the more nucleophilic metallic centers among these series. For instance, a 16 cm^{-1} shift towards lower frequencies is observed in the IR spectra for complexes **3** and **4** when compared to those shown by related amido complexes [{M(μ-NH{*p*-tolyl})$(CO)_2$}$_2$] (M = Rh, Ir).[29] The simple and effective NH_2-bridged bimetallic system should be responsible by itself of the high basicity induced to the metals.

This scenario has been explored by assessing the reactivity of iridium complex **2** with chlorocarbons, which are known to be relatively unreactive substrates and are indeed used as solvents in many organometallic reactions. Rhodium complex **1** was found to be very reactive towards chloroform and dichloromethane giving, among unidentifiable mixtures of COD-containing complexes and black insoluble solids, yellow crystals of the mononuclear ammine adduct [Rh(cod)Cl(NH_3)], which was fully characterized (see the Supporting Information). More interestingly, the iridium complex **2** reacted in a controlled way towards selected chlorocarbons (CH_2Cl_2, $CHCl_3$, and $ClCH_2CH_2Cl$), affording in general dinuclear adducts that arise from a concerted dinuclear oxidative addition of the substrates.

NMR monitoring of the reaction of **2** with a tenfold excess of dichloromethane or chloroform in [D_6]benzene solutions in the absence of light showed, after a few days, the complete transformation to new species characterized as the dinuclear adducts [(Cl)(cod)Ir(μ-NH_2)$_2$Ir(cod)(CH_2Cl)] (**5**) and [(Cl)(cod)Ir(μ-NH_2)$_2$Ir(cod)($CHCl_2$)] (**6**), respectively. However, when dichloroethane was used as substrate, the clean formation of the symmetrical di-chloro complex [{Ir(μ-NH_2)(cod)(Cl)}$_2$] (**7**) was observed, along with released ethylene (Scheme 2). The diiridium adducts **5**–**7** were fully characterized by multinuclear NMR spectroscopy, including ^{15}N–^{1}H HMBC, ^{13}C–^{1}H HSQC, and COSY bidimensional techniques, mass spectrometry, IR spectroscopy, and elemental analyses.

Red single crystals of complexes **5** and **7** were obtained by allowing concentrated solutions of complex **2** to stand in toluene with dichloromethane or dichloroethane for three days, respectively. X-ray diffraction measurements confirmed the dinuclear nature of adducts **5** and **7**, and revealed the fact that the asymmetric unit of **7** is composed by two crystallographically independent but very similar molecules (together with two solvent toluene molecules). For clarity, only one of them will be described in this manuscript, further information can be found in the Supporting Information.

The molecular structures of **5** and **7** are depicted in Figures 4 and 5, respectively. Selected bond length and angles are given in Tables 4 and 5, respectively. Both complexes show a similar dinuclear arrangement, with iridium centers linked together by two parent amido groups. Without considering metal–metal bonds, the geometry around the metal atoms is best described as a slightly distorted square pyramid. In both complexes the pyramid base is formed by the olefinic carbon atoms of the cyclooctadiene ligand (coordi-

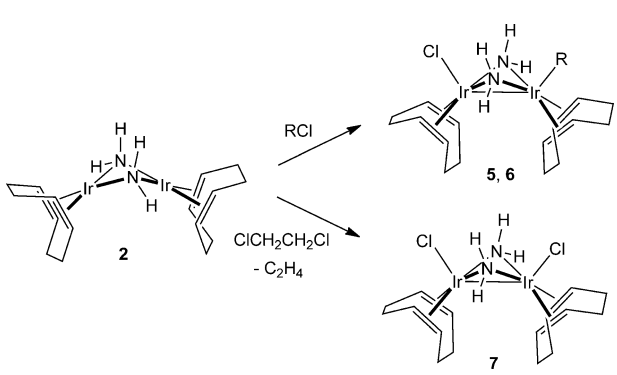

Scheme 2. Synthesis of the dinuclear adducts **5**–**7**; R = CH_2Cl (**5**), $CHCl_2$ (**6**).

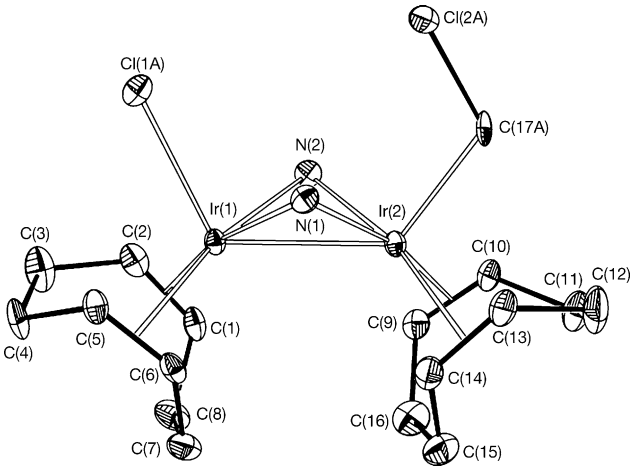

Figure 4. Molecular structure of complex **5**.

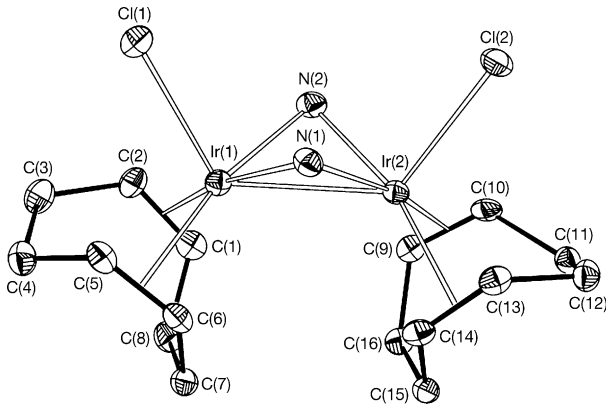

Figure 5. Molecular structure of complex **7**.

Table 4. Selected bond lengths [Å] and angles [°] for complex **5**.[a]

Ir(1)–Ir(2)	2.6794(3)	Ir(1)–Cl(1A)	2.516(3)
Ir(1)–N(1)	2.078(5)	Ir(2)–N(1)	2.043(5)
Ir(1)–N(2)	2.064(5)	Ir(2)–N(2)	2.054(5)
Ir(1)–M(1)	2.032(6)	Ir(2)–M(3)	2.037(6)
Ir(1)–M(2)	2.044(6)	Ir(2)–M(4)	2.040(6)
Ir(2)–C(17A)	2.148(12)	C(17A)–Cl(2A)	1.819(12)
C(1)–C(2)	1.403(8)	C(9)–C(10)	1.398(8)
C(5)–C(6)	1.394(8)	C(13)–C(14)	1.397(8)
Cl(1A)-Ir(1)-N(1)	83.44(16)	C(17A)-Ir(2)-N(1)	90.4(4)
Cl(1A)-Ir(1)-N(2)	86.98(15)	C(17A)-Ir(2)-N(2)	93.8(3)
N(1)-Ir(1)-N(2)	78.2(2)	N(1)-Ir(2)-N(2)	79.3(2)
N(1)-Ir(1)-M(1)	166.1(2)	N(1)-Ir(2)-M(3)	167.2(2)
N(1)-Ir(1)-M(2)	98.2(2)	N(1)-Ir(2)-M(4)	94.6(2)
N(2)-Ir(1)-M(1)	94.7(2)	N(2)-Ir(2)-M(3)	96.8(2)
N(2)-Ir(1)-M(2)	168.1(2)	N(2)-Ir(2)-M(4)	167.0(2)

[a] M(1), M(2), M(3), and M(4) represent the midpoints of the C(1)–C(2), C(5)–C(6), C(9)–C(10), and C(13)–C(14) olefinic bonds, respectively.

Table 5. Selected bond lengths [Å] and angles [°] for complex **7**.[a]

Ir(1)–Cl(1)	2.4344(11)	Ir(2)–Cl(2)	2.4565(10)
Ir(1)–N(1)	2.060(3)	Ir(2)–N(1)	2.053(3)
Ir(1)–N(2)	2.059(3)	Ir(2)–N(2)	2.062(4)
Ir(1)–-M(1)	2.045(4)	Ir(2)-–M(3)	2.040(4)
Ir(1)–M(2)	2.055(4)	Ir(2)–M(4)	2.035(5)
C(1)–C(2)	1.392(6)	C(9)–C(10)	1.401(6)
C(5)–C(6)	1.394(6)	C(13)–C(14)	1.396(6)
Ir(1)–Ir(2)	2.6544(2)		
Cl(1)-Ir(1)-N(1)	87.13(10)	Cl(2)-Ir(2)-N(1)	87.56(10)
Cl(1)-Ir(1)-N(2)	87.85(11)	Cl(2)-Ir(2)-N(2)	89.74(11)
N(1)-Ir(1)-N(2)	78.88(14)	N(1)-Ir(2)-N(2)	78.97(14)
N(1)-Ir(1)-M(1)	167.91(15)	N(1)-Ir(2)-M(3)	167.80(15)
N(1)-Ir(1)-M(2)	96.17(15)	N(1)-Ir(2)-M(4)	95.24(15)
N(2)-Ir(1)-M(1)	96.43(15)	N(2)-Ir(2)-M(3)	96.24(16)
N(2)-Ir(1)-M(1)	167.66(15)	N(2)-Ir(2)-M(4)	165.36(15)

[a] M(1), M(2), M(3), and M(4) represent the midpoints of the C(1)–C(2), C(5)–C(6), C(9)–C(10), and C(13)–C(14) olefinic bonds, respectively.

nated in their typical η^2-C=C mode) and the nitrogen atoms of the amido groups. The apical position of one of the iridium atoms is occupied by a chlorine, whereas a carbon atom of a chloromethylene fragment (**5**) or a chlorine (**7**) is located at the apex of the other pyramid.

The square pyramids of both metal atoms share the basal edge defined by the two amido groups, allowing this way the formation of iridium–iridium bonds (Ir(1)–Ir(2): 2.6794(3) and 2.6544(2) Å for complex **5** and **7**, respectively). These short separations fall within the range of iridium–iridium bond lengths, and are comparable to those observed in related dinuclear, metal–metal bonded complexes such as [{Ir(μ-S*t*Bu)(I)(CO)$_2$}$_2$] (2.638(1) Å; *t*Bu = *tert*-butyl),[33] [{Ir(μ-Pz)-(μ-S*t*Bu)(μ-dmad)(P(OMe)$_3$)$_2$(CO)$_2$}$_2$] (2.614(2) Å; Pz = pyrazolyl, dmad = dimethylacetylenedicarboxylate),[34] or [{Ir(μ-NCPh$_2$)Cl(cod)}$_2$] (2.6829(7) Å).[35]

The presence of iridium–iridium bonds in these adducts necessarily results too from an electronic perspective, because it accounts for their diamagnetism, as confirmed by NMR measurements, and therefore can be formally considered as oxidized Ir^{II}–Ir^{II} entities. As a matter of fact, the symmetrical complex **7** gave two different resonances for the cod=CH protons in the ^{1}H NMR spectrum, clearly reflecting the C_{2v} symmetry observed in the solid state, whereas the non-symmetrical adducts **5** and **6** gave four distinct signals both in their ^{1}H and their ^{13}C{^{1}H} NMR spectra, in accordance with the C_s symmetry found in the molecular structure of **5**.

Some comments concerning the formation of the oxidized species **5**–**7** should be underlined at this point. Although two-center oxidative addition of chloro-containing substrates is a process well recognized in some diiridium systems with highly basic ancillary such as isocyanides,[36] the action of light (or ultraviolet light) is frequently needed.[37] For the sake of comparison, the diiridium pyrazolyl complex [Ir(μ-Pz)(cod)]$_2$ is stable for weeks in dichloromethane or dichloroethane; however, in the presence of visible irradiation it undergoes a four-electron substrate reduction to give well-defined oxidized species.[38]

Amido phosphane and N-heterocyclic carbene complexes: Encouraged by the lack of late d^8 metal parent amido complexes reported up to date, we took advantage of the ready availability of amido complexes of Rh^I and Ir^I through our original synthetic protocol to explore their reactivity. In particular, we chose different phosphanes and the N-heterocyclic carbene 1,3-bis(2,6-diisopropylphenyl)imidazol-2-ylidene (IPr) as external ligands in an attempt to establish the strength of the amido bridges in complexes **1** and **2**.

The dirhodium complex **1** reacted with all selected phosphanes PR$_3$ (PR$_3$ = PPh$_3$, PMePh$_2$, PMe$_2$Ph) by replacing the cyclooctadiene ligands in a stepwise manner, without splitting of the amido bridges. NMR experiments allowed us to observe, upon addition of two molar equivalents of the respective phosphanes to **1**, free COD and the formation of mixed di-olefin/bis(phosphane) dinuclear species [(cod)Rh-(μ-NH$_2$)$_2$Rh(PR$_3$)$_2$] (PR$_3$ = PPh$_3$ (**8**), PMePh$_2$ (**9**), PMe$_2$Ph (**10**)), with an observed COD/PR$_3$ ratio in their ^{1}H NMR spectra of 1:2 in all cases. The NMR pattern of the COD protons and carbons at all ranges of temperature indicated C_{2v} symmetry, instead of the expected C_s symmetry related with an open-book-like geometry (see the Experimental Section). To fully understand the NMR spectra of complexes **8**–**10** one has to consider the known butterfly-like motion associated with dinuclear amido-bridged d^8 complexes, which consists of a four-membered metallacycle inversion, which is very fast on the NMR time scale. This dynamic process produces averaged NMR signals that reflect a planar "RhNRhN" core, a situation that has only been found for two diarylamido-bridged rhodium complexes of the type [{Rh(μ-NAr$_2$)(cod)}$_2$] (Ar = phenyl, *p*-tolyl), because it is the most stable situation in terms of the avoidance of steric contacts between the sterically demanding aryl amido and COD ligands.[39]

Further addition of two extra molar equivalents of the respective phosphanes afforded tetraphosphane complexes [{Rh(μ-NH$_2$)(PR$_3$)$_2$}$_2$] (PR$_3$ = PPh$_3$ (**11**), PMePh$_2$ (**12**), PMe$_2$Ph (**13**)), which were isolated as brown–reddish solids in fairly good yields (Scheme 3). The NMR spectra of **11**–**13**

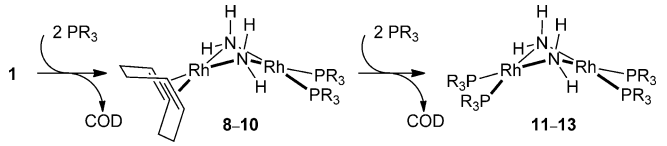

Scheme 3. Synthesis of the mixed COD/phosphane complexes **8–10** ($PR_3 = PPh_3$ (**8**), $PMePh_2$ (**9**), PMe_2Ph (**10**)), and the tetraphosphane complexes **11–13** ($PR_3 = PPh_3$ (**11**), $PMePh_2$ (**12**), PMe_2Ph (**13**)).

showed phosphane and amido resonances in a 2:1 ratio, and their dinuclear nature was confirmed by mass spectrometry. In all phosphane complexes **8–13**, the NH_2 resonances were observed at high field (from $\delta = -0.30$ to -0.78 ppm) in the ^{1}H NMR spectra, which correlated with amido nitrogen atoms ($\delta(^{15}N) = -5.1$ to -17.8 ppm), in which the more negative value corresponds to the more basic phosphane. Disappointingly, no terminal amido complexes of rhodium of the type $[Rh(NH_2)(PR_3)_3]$ were detected by NMR techniques, regardless of the amount of added phosphane. This situation is in marked contrast when aryl amido ligands are involved: in these cases, the related dinuclear complexes $[\{Rh(\mu\text{-}NArH)_2(PEt_3)_2\}_2]$ (NArH = *p*-toluidine, *p*-anisidide, *o*-anisidide, *p*-trifluoromethylanilide) do react with an excess of triethylphosphane to form the reactive terminal amido species $[Rh(NArH)(PEt_3)_3]$.[40] This situation may be tentatively explained by considering that NH_2 ligands do not bear electron-withdrawing groups that could help to stabilize such electron-rich terminal amido species, as it happens when aryl amido ligands are involved.

Turning our attention to iridium, when complex **2** was reacted with PPh_3, PMe_2Ph, or even PMe_3, insoluble intractable mixtures of phosphorous-containing complexes were formed, which were not further characterized. Only when the phosphane $PMePh_2$ was reacted in situ with complex **2** in $[D_6]$benzene, we observed the formation of a novel terminal amido complex $[Ir(cod)(NH_2)(PMePh_2)_2]$ (**14**). This amido derivative evolved to the hydroxo complex $[Ir(cod)(OH)(PMePh_2)_2]$ (**15**) along with released ammonia in wet solvents, as observed by NMR techniques (Scheme 4).

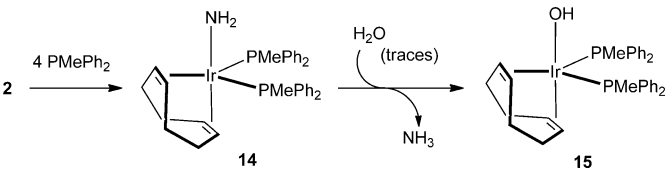

Scheme 4. Proposed structure for the terminal amido complex **14**, and its conversion to the terminal hydroxo complex **15**.

The ^{1}H NMR spectrum of **14** in $[D_6]$benzene showed a significant broad resonance at high field ($\delta = -0.83$ ppm) assigned to the NH_2 group; whereas at room temperature the =CH protons of the COD ligand were observed as a sole resonance, at $-40\,^\circ$C they split into two distinct resonances. Very importantly, the $PMePh_2$/COD/NH_2 ratio found was 2:1:1. The presence of a broad singlet in the $^{31}P\{^1H\}$ NMR spectrum for the symmetrical phosphanes in **14** together with the information gathered from the ^{1}H and $^{13}C\{^1H\}$ NMR spectra suggested a mononuclear penta-coordinated complex with C_s symmetry, in principle coherent with a trigonal-bipyramidal (tbp) structure. This information was further confirmed by the micro-TOF mass spectrum of **14**, which showed a peak at *m/z* 717.1997 with the exact isotopic distribution for the $[Ir(cod)(NH_2)(PMePh_2)_2]^+$ ion.

Although we were not able to locate the nitrogen signal by ^{15}N–^1H HMBC experiments in the amido complex **14**, the presence of a NH_2 group coordinated to iridium was confirmed indirectly by its chemical reactivity: as expected, addition of stoichiometric amounts of water to a solution of **14** in $[D_6]$benzene gave rise to the clean transformation to the hydroxo complex **15** and released ammonia. This conversion was irreversible, because exposure of **15** to ammonia does not revert back the reaction to the amido complex **14**. All the attempts made in order to isolate the amido complex **14** were fruitless, because it was found to be highly reactive towards moisture (traces). Instead, we isolated the hydroxo analogue $[Ir(cod)(OH)(PMePh_2)_2]$ (**15**), which is much more stable than its amido precursor. The NMR spectra of **15** were virtually similar to those of the amido complex **14**, so both complexes should be isostructural. Furthermore, variable temperature NMR data of **15** indicated the existence of a fluxional process that could be slowed down at $-40\,^\circ$C in $[D_8]$toluene, leading to the splitting of the =CH COD protons (as observed with the amido complex **14**), in accordance to the proposed penta-coordinated structure, as depicted in Scheme 4: both symmetrical phosphanes are located at the equatorial positions of a tbp, whereas the strong donor OH (or NH_2) group is located at the axial site, *trans* to one of the C=C olefinic bonds. According to this, irradiation at the hydroxo signal ($\delta = -2.71$ ppm) gave a strong positive NOE effect with the equatorial =CH protons of the COD ligand.

Having in mind the success on isolating the first terminal parent amido complexes of rhodium by utilizing the electron-withdrawing di-olefin tetrafluorobenzobarrelene and IPr as a voluminous and strong σ-donor N-heterocyclic carbene ligand,[20] we explored in the same way the splitting of the amido bridges in complexes **1** and **2** with IPr. When **1** was treated with two molar equivalents of IPr, a yellow microcrystalline solid was isolated in excellent yield. Further inspection of its ^{1}H NMR spectrum showed quite unexpectedly that it corresponded to the recently reported terminal hydroxo complex $[Rh(cod)(IPr)(OH)]$.[41] In the same way, reaction of iridium complex **2** with IPr afforded the novel hydroxo complex $[Ir(cod)(IPr)(OH)]$ (**17**) in high yield, which was characterized by NMR spectroscopy, mass spectrometry, and elemental analysis.

These terminal hydroxo species should have their origin from hydrolysis of too reactive transient terminal amido species $[M(cod)(IPr)(NH_2)]$ (Scheme 5). As a matter of fact, NMR monitoring of the reaction of iridium complex **2** with IPr at low temperatures allowed to detect the amido intermediate $[Ir(cod)(IPr)(NH_2)]$ (**16**), which was characterized

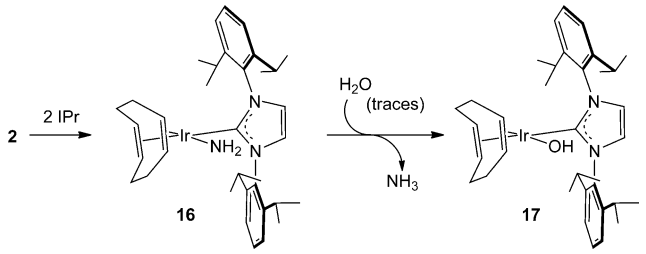

Scheme 5. Formation of the hydroxo complex **17** through the terminal amido intermediate [Ir(cod)(IPr)(NH_2)] (**16**).

in [D_6]benzene: the pattern of the ^{1}H NMR spectrum was virtually identical to that of the hydroxo analogue **17**, showing two signals for the =CH COD protons and a broad resonance for the NH_2 protons, whereas the COD/IPr/NH_2 ratio found was 1:1:1. These amido species **16** gradually converted to hydroxo complex **17** along with released ammonia within several hours, a transformation that can be slowed down by lowering the temperature. Nevertheless, even when using carefully amalgam-dried solvents, the amido species proved to be too reactive towards moisture to be isolated. In this way, the splitting of the amido bridges in complexes **1** and **2** by IPr gives the expected terminal amido species [(cod)M(IPr)(NH_2)], similarly to those reported with tfbb (tfbb = tetrafluorobenzobarrelene); however, the COD ancillary ligand is much less π acid than fluorinated tfbb, a situation that helps to understand the sensitiveness of terminal amido COD complexes towards hydrolysis. This phenomenon has been already reported in some terminal amido ruthenium complexes, a behavior sometimes compared to that of strong basic alkaline amides.[1a]

Nevertheless, it is interesting to notice that reports of stable terminal hydroxo late-metal complexes are rare,[22] and quite often hydroxo alkali chemicals are required for their preparation from chloro-containing metallic precursors. The preparative method described here takes advantage of the high tendency towards hydrolysis of terminal amido complexes, and it could be the synthetic method of choice, because it utilizes water as the hydroxo source and releases gaseous ammonia as the only byproduct, avoiding this way the use of strong bases and salt removal.

Catalytic activity of the cyclooctadiene complexes 1 and 2 in the transfer hydrogenation of acetophenone: In a preliminary communication we reported that complex **2**, at room temperature and in absence of any base, was active as homogeneous catalysts for the transfer hydrogenation of acetophenone to 1-phenylethanol by using *i*PrOH as hydrogen donor. Under such mild conditions a bimetallic mechanism that allows a concerted net hydrogen transfer through a proposed eight-membered dimetallacycle was proposed.[25] However, the catalytic activity was relatively low and, in the absence of acetophenone, or when its concentration was substantially decreased, the formation of a stable imido cluster of the formula [Ir_3(cod)$_3$(μ_2-H)(μ_3-NH)$_2$] was observed.

We have now tested, at 80 °C, the catalytic performance for the hydrogen transfer of the iridium and rhodium cyclooctadiene parent amido complexes **2** and **1**, in the absence of any base and in the presence of cesium carbonate. The addition of a weak base in the catalytic system was beneficial in the case of the iridium catalyst **2**, because in the presence of 3 mol% of cesium carbonate, almost quantitative conversions to 1-phenylethanol was obtained after 24 h, this was an improvement from 48% without base to 94% with Cs_2CO_3. However, with the analogous rhodium complex **1**, conversions were less efficient and no positive effect was observed with added Cs_2CO_3.

The time dependence for the transfer hydrogenation processes of acetophenone by using complexes **1** and **2** as catalysts in the presence of 3 mol% Cs_2CO_3 was monitored during 24 h. As illustrated in Figure 6, the iridium catalyst was more active than the rhodium analogue, which showed only moderate activity. As a matter of fact, the turn over frequency at 50% conversion (TOF_{50})[23] for iridium catalyst **2** was approximately 1880 h^{-1}, whereas the rhodium catalyst **1** gave a much lower TOF_{50} of 27 h^{-1}.

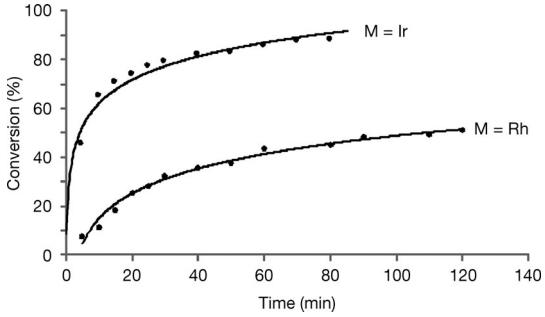

Figure 6. Time dependence for the transfer hydrogenation of acetophenone by using 1 mol% of complexes **1** or **2** as catalysts at 80 °C and 3 mol% Cs_2CO_3 as external base.

The role of the cesium carbonate is not really clear at this point. We selected it because is a very weak base (as compared with the strong base *t*BuOK, usually utilized in these processes to deprotonate *i*PrOH) and therefore it is possible to speculate about a conventional deprotonation of isopropanol to yield hydrido metal species that should be involved in the classical hydrido mechanism, or alternatively the cesium ion could interact with the iridium centers in the pocket of the open-book dinuclear structure improving the activity of the bimetallic species. In any case, the presence of a weak base as cesium carbonate, considerably improves the activity of the iridium catalyst for the transfer hydrogenations.

Conclusion

In this contribution we have explored the chemistry around unusual parent amido complexes of the type [{M(μ-NH_2)(cod)}$_2$] (M = Rh, Ir). In general, the amido ligands act as tight bridges without compromising the dinuclear entity such as in di-olefin replacement reactions with carbon mon-

oxide. The diiridium(I) complex $[\{Ir(\mu\text{-}NH_2)(cod)\}_2]$ activates chloroalkanes giving diiridium(II) products as a result of a two-center oxidative addition and concomitant metal–metal bond formation. The $[\{M(\mu\text{-}NH_2)(cod)\}_2]$ complexes react with phosphanes; in the case of rhodium, phosphanes are not able to split the amido bridges, allowing the detection of mixed COD/phosphane dinuclear complexes $[(cod)Rh(\mu\text{-}NH_2)_2Rh(PR_3)_2]$, and the isolation of the respective tetraphosphanes $[\{Rh(\mu\text{-}NH_2)(PR_3)_2\}_2]$. However, we observed splitting of the amido bridges when iridium is involved: this system efficiently generates a novel terminal amido complex of Ir^I, which is too reactive to be isolated. Likewise, the carbene IPr allowed the access to very reactive terminal amido complexes, detectable only in the case of iridium at low temperatures. These species evolve through hydrolysis to stable terminal hydroxo complexes, even with traces of moisture. The $[\{M(\mu\text{-}NH_2)(cod)\}_2]$ complexes are active homogeneous catalysts for the transfer hydrogenation of acetophenone to 1-phenylethanol by using *i*PrOH as hydrogen donor, the iridium catalyst being more active than the rhodium analogue, which showed only moderate activity.

Experimental Section

General methods: All manipulations were performed under a dry argon atmosphere by using Schlenk-tube techniques. Solvents were obtained from a solvent purification system (Innovative Technologies) or were dried by standard procedures and distilled under argon prior to use. Complexes **1** and **2** were prepared by following the synthetic procedure recently described.[20] Gaseous ammonia was purchased from Air Liquide LTD. All the other chemicals used in this work have been purchased from Aldrich Chemicals and were used as received. Carbon, hydrogen, and nitrogen analyses were performed with a Perkin–Elmer 2400 CHNS/O microanalyzer. Mass spectra were recorded on a VG Autospec double-focusing mass spectrometer operating in the FAB^+ mode. Ions were produced with the standard Cs^+ gun at approximately 30 kV; 3-nitrobenzyl alcohol (NBA) was used as matrix. ESI MS was recorded on a Bruker Micro-Tof-Q by using sodium formiate as reference. ^1H, $^{31}P\{^1H\}$, and $^{13}C\{^1H\}$ NMR spectra were recorded on a Varian UNITY, a Bruker ARX 300, and a Bruker Avance 400 spectrometers operating at 299.95, 121.42, and 75.47 MHz, 300.13, 121.49 and 75.47 MHz, and 400.13, 161.99 and 100.00 MHz, respectively. Chemical shifts are reported in [ppm] and referenced to Me_4Si by using the residual signal of the deuterated solvent (^1H and ^{13}C), H_3PO_4 as external reference (^{31}P) and liquid NH_3 (^1H–^{15}N HMQC). IR spectra were recorded in solution on a Perkin–Elmer Spectrum One spectrometer by using a cell with NaCl windows.

Synthesis of $[\{Rh(\mu\text{-}NH_2)(CO)_2\}_2]$ (3): Carbon monoxide was bubbled through a yellow solution of **1** (0.18 g, 0.40 mmol) in toluene (10 mL) at room temperature giving a brownish solution. The bubbling was continued for 30 min, and then hexane (20 mL) was added to induce the precipitation of a yellow solid, which was collected by filtration through a cannula, washed with hexane, and dried under vacuum (0.07 g, 50%). ^1H NMR (300 MHz, [D$_6$]benzene): $\delta = -1.40$ ppm (br s, 4H; NH_2); $^{13}C\{^1H\}$ NMR (75 MHz, [D$_6$]benzene): $\delta = 187.0$ ppm (d, $^1J(C,Rh) = 64$ Hz, CO); ^{15}N–^1H HMQC (41 MHz, [D$_6$]benzene): $\delta = -45.0$ ppm (br s, NH_2); IR (THF): $\tilde{\nu} = 2079, 2042, 1970$ (CO), 3369 cm^{-1} (NH_2); elemental analysis calcd (%) for $C_4H_4N_2O_4Rh_2$: C 13.73, H 1.15, N 8.01; found: C 14.56, H 1.07, N 7.75.

Synthesis of $[\{Ir(\mu\text{-}NH_2)(CO)_2\}_2]$ (4): Carbon monoxide was bubbled through a red solution of **2** (0.10 g, 0.16 mmol) in toluene (10 mL) at room temperature giving a deep green solution. The bubbling was continued for 30 min, and then hexane (20 mL) was added to induce the precipitation of a dark green solid, which was collected by filtration through a cannula. Recrystallization of the crude dark solid with benzene gave yellow crystals of **4** (0.06 g, 63%). ^1H NMR (300 MHz, [D$_6$]benzene): $\delta = -0.25$ ppm (br s, 4H; NH_2); $^{13}C\{^1H\}$ NMR (75 MHz, [D$_6$]benzene): $\delta = 175.8$ ppm (s, CO); ^{15}N–^1H HMQC (40 MHz, [D$_6$]benzene): $\delta = 5.1$ ppm (br s, NH_2); ESI MS (μ-TOF+): m/z: 266.5 $[M^+/2+H]$; IR (THF): $\tilde{\nu} = 2059, 2035, 1972$ (CO), 3393 cm^{-1} (NH_2); elemental analysis calcd (%) for $C_4H_4Ir_2N_2O_4$: C 9.09, H 0.76, N 5.30; found: C 9.03, H 0.72, N 5.24.

Synthesis of $[(Cl)(cod)Ir(\mu\text{-}NH_2)_2Ir(cod)(CH_2Cl)]$ (5): Complex **2** (0.10 g, 0.16 mmol) was dissolved in toluene (10 mL) and then neat dichloromethane (0.14 g, 104 μL, 1.64 mmol) was added through a microsyringe. The deep red solution was stirred for a week at RT under dark. At this point, the solution was filtered through a cannula and the solvent was removed by vacuum to approximately 2 mL. Addition of hexane afforded a red solid, which was collected by filtration, washed with hexane, and then dried in vacuum (69 mg, 51%). ^1H NMR (300 MHz, $CDCl_3$): $\delta = 5.26$ (s, 2H; CH_2Cl), 3.98 (m, 2H), 3.81 (m, 2H), 3.70 (m, 2H), 3.55 (m, 2H; = CH COD), 3.45 (br s, 2H; NH_2), 2.75 (m, 2H; CH_2 COD), 2.68 (br s, 2H; NH_2), 2.62 (m, 2H), 2.50 (m, 2H), 2.41 (m, 2H), 2.23 ppm (m, 8H; CH_2 COD); $^{13}C\{^1H\}$ NMR (75 MHz, $CDCl_3$): $\delta = 77.6$ (s), 72.3 (s), 70.8 (s), 65.6 (s, =CH), 35.0 (s), 32.5 (s), 30.4 (s), 30.2 (s, CH_2 COD), −2.4 ppm (s, CH_2Cl); ^{15}N–^1H HMQC (40 MHz, $CDCl_3$): $\delta = 16.7$ ppm (br s, NH_2); ESI MS (μ-TOF+): m/z: 683.13 $[M^+-Cl+H]$; IR (solid): $\tilde{\nu} = 3343$ cm^{-1} (NH_2); elemental analysis calcd (%) for $C_{17}H_{30}Cl_2Ir_2N_2$: C 28.45, H 4.21, N 3.90; found: C 28.64, H 4.01, N 3.92.

Synthesis of $[(Cl)(cod)Ir(\mu\text{-}NH_2)_2Ir(cod)(CHCl_2)]$ (6): To a solution of complex **2** (0.04 g, 0.06 mmol) in toluene (3 mL), neat chloroform (0.08 g, 51 μL, 0.63 mmol) was added through a microsyringe and the mixture was allowed to stir overnight at room temperature in the absence of light. The resulting deep brown solution was filtered through a cannula and the solvent was removed in vacuum to approximately 2 mL. Addition of hexane afforded a yellow solid, which was collected by filtration, washed with hexane, and then dried in vacuum (40 mg, 84%). ^1H NMR (300 MHz, $CDCl_3$): $\delta = 7.58$ (s, 1H; $CHCl_2$), 4.09 (m, 2H), 3.95 (m, 2H), 3.90 (m, 2H), 3.68 (m, 2H) (CH_2 COD), 3.40 (br s, 2H), 3.19 (br s, 2H; NH_2), 2.78 (m, 2H), 2.66 (m, 2H), 2.57 (m, 2H), 2.50 (m, 2H), 2.37 ppm (m, 8H; CH_2 COD); $^{13}C\{^1H\}$ NMR (75 MHz, $CDCl_3$): $\delta = 80.1$ (s), 74.4 (s), 72.7 (s), 70.9 (s, =CH), 34.8 (s), 33.7 (s), 30.8 (s), 29.8 ppm (s, CH_2, COD); ^{15}N–^1H HMQC (40 MHz, CD_2Cl_2): $\delta = 17.1$ ppm (br s, NH_2); ESI MS (μ-TOF+): m/z: 716.9 $[M^+-Cl]$; IR (solid): $\tilde{\nu} = 3343$ cm^{-1} (NH_2); elemental analysis calcd (%) for $C_{17}H_{29}Cl_3Ir_2N_2$: C 27.14, H 3.89, N 3.72; found: C 27.79, H 4.00, N 3.87.

Synthesis of $[\{Ir(\mu\text{-}NH_2)(cod)(Cl)\}_2]$ (7): A solution of **2** (0.04 g, 0.06 mmol) in toluene (3 mL) was treated with neat dichloroethane (0.06 g, 50 μL, 0.63 mmol) through a microsyringe, and then allowed to stir overnight at room temperature in the absence of light. The deep red solution formed was filtered through a cannula and then the solvent was removed in vacuum to approximately 2 mL. Addition of hexane afforded a red solid, which was collected by filtration, washed with hexane, and then dried in vacuum (40 mg, 89%). ^1H NMR (300 MHz, $CDCl_3$): $\delta = 4.51$ (m, 4H), 4.14 (m, 4H) (=CH COD), 3.87 (br s, 2H), 3.69 (br s, 2H; NH_2), 2.89 (m, 2H), 2.64 (m, 2H), 2.58 (m, 2H), 2.32 ppm (m, 2H; CH_2 cod); $^{13}C\{^1H\}$ NMR (75 MHz, $CDCl_3$): $\delta = 78.0$ (s), 77.5 (s, =CH), 34.3 (s), 30.8 ppm (s, CH_2, COD); ^{15}N–^1H HMQC (40 MHz, $CDCl_3$): $\delta = 16.9$ ppm (br s, NH_2); ESI MS (μ-TOF+): m/z: 669.12 $[M^+-Cl+H]$; IR (solid): $\tilde{\nu} = 3343$ cm^{-1} (NH_2); elemental analysis calcd (%) for $C_{16}H_{28}Cl_2Ir_2N_2$: C 27.31, H 4.01, N 3.98; found: C 26.93, H 3.81, N 3.74.

Synthesis of $[(cod)Rh(\mu\text{-}NH_2)_2Rh(PPh_3)_2]$ (8): An NMR tube was charged with complex **1** (13 mg, 0.03 mmol) and the solid was dissolved in deoxygenated [D$_6$]benzene. Solid triphenylphosphane (44 mg, 0.17 mmol) was added to this solution and then allowed to react for 1 h. At this point, the conversion to **8** was quantitative. ^1H NMR (300 MHz, [D$_6$]benzene): $\delta = 7.96$ (m, 12H; H_o), 7.15 m, 18H; $H_m + H_p$, PPh_3), 3.64 (m, 4H;=CH), 2.56 (m, 4H), 1.98 (m, 4H; CH_2 COD), −0.78 ppm (br s, 4H; NH_2); $^{31}P\{^1H\}$ NMR (121 MHz, [D$_6$]benzene): $\delta = 51.3$ ppm (d, $^1J(P,Rh) = 173$ Hz); $^{13}C\{^1H\}$ NMR (75 MHz, [D$_6$]benzene): $\delta = 138.0$ (d, $^1J(C,Rh) = 40$ Hz, C_{ipso}), 134.7 (m, C_o), 128.8 (m, $C_m + C_p$, PPh_3), 73.8 (d,

^1J(C,Rh) = 12 Hz, =CH), 31.9 (s), 28.2 ppm (s, CH_2 COD); ^{15}N–^{1}H HMQC (40 MHz, [D_6]benzene): $\delta = -5.1$ ppm.

Synthesis of [(cod)Rh(μ-NH_2)$_2$Rh($PMePh_2$)$_2$] (9): An NMR tube was charged with complex **1** (30 mg, 0.06 mmol) and the solid was dissolved in deoxygenated [D_6]benzene. Pure methyldiphenylphosphane (0.03 g, 25 μL, 0.13 mmol) was added to this solution through a microsyringe and then allowed to stand for 5 min. At this point, the conversion to **9** was quantitative. ^{1}H NMR (300 MHz, [D_6]benzene): $\delta = 7.78$ (m, 8H; H_o), 7.18–6.97 (m, 12H; $H_m + H_p$, PPh_2), 3.64 (m, 4H; =CH), 2.57 (m, 4H), 2.00 (m, 4H, CH_2 COD), 1.45 (m, 6H; PMe), −0.77 ppm (brs, 4H; NH_2); ^{31}P{^{1}H} NMR (121 MHz, [D_6]benzene): $\delta = 31.1$ ppm (d, ^1J(P,Rh) = 167 Hz); ^{13}C{^{1}H} NMR (75 MHz, [D_6]benzene): $\delta = 140.8$ (m, C_{ipso}), 132.8 (m, C_o), 127.5–128.1 (m, $C_m + C_p$, PPh_2), 73.7 (d, ^1J(P,Rh) = 12 Hz, =CH), 31.9 (s), 28.2 (s, CH_2 COD), 17.6 (d, ^2J(C,P) = 14 Hz), 17.4 ppm (d, ^2J-(C,P) = 14 Hz, PMe); ^{15}N–^{1}H HMQC (40 MHz, [D_6]benzene): $\delta = -8.8$ (brs,, NH_2); ESI MS (MALDI+): *m/z*: 635.7 [M^+−COD−3H], 542.0 [M^+−$PMePh_2$−4H).

Synthesis of [(cod)Rh(μ-NH_2)$_2$Rh(PMe_2Ph)$_2$] (10): Complex **10** was prepared in situ by following the procedure described for complex **9**, by reacting **1** (0.02 g, 0.05 mmol) and dimethylphenylphosphane (0.01 g, 16 μL, 0.11 mmol) in [D_6]benzene. ^{1}H NMR (300 MHz, [D_6]benzene): $\delta = 8.10$ (m, 4H; C_o), 7.14–7.32 (m, 6H; $H_m + H_p$, PPh), 3.88 (m, 4H; =CH), 2.72 (m, 4H), 2.15 (m, 4H; CH_2 COD), 1.31 (m, 12H; PMe_2), −0.46 ppm (brs, 4H; NH_2); ^{31}P{^{1}H} NMR (121 MHz, [D_6]benzene): $\delta = 13.4$ ppm (d, ^1J(P,Rh) = 170 Hz); ^{13}C{^{1}H} NMR (75 MHz, [D_6]benzene): $\delta = 142.9$ (d, ^1J(P,Rh) = 34 Hz, C_{ipso}), 131.2 (m, C_o), 128.5, 128.4 127.6–127.4 (set of s, $C_m + C_p$, PPh), 73.7 (d, ^1J(C,Rh) = 12 Hz, =CH), 31.8 (s), 28.1 (s) (, CH_2 COD), 19.0 (d, ^2J(C,P) = 13 Hz), 18.8 ppm (d, ^2J(C,P) = 13 Hz, PMe_2); ^{15}N–^{1}H HMQC (40 MHz, [D_6]benzene): $\delta = -11.6$ ppm (brs, NH_2); MS (ESI+): *m/z*: 394.9 [M^+−Rh−NH_2−COD].

Synthesis of [{Rh(μ-NH_2)(PPh_3)$_2$}$_2$] (11): A solution of complex **1** (0.10 g, 0.22 mmol) in toluene (9 mL) was treated with solid triphenylphosphane (0.35 g, 1.32 mmol) and the resulting mixture was stirred for 2 h. The volatiles were removed in vacuum leaving an orange solid, which was recrystallized from toluene and hexane (0.19 g, 67%). ^{1}H NMR (300 MHz, [D_6]benzene): $\delta = 7.75$ (m, 24H; H_o), 7.02 (m, 24H; H_m), 6.81 (m, 12H; H_p, PPh_3), −2.01 ppm (br s, 4H; NH_2); ^{31}P{^{1}H} NMR (121 MHz, [D_6]benzene): $\delta = 57.2$ ppm (d, ^1J(P,Rh) = 187 Hz); ^{13}C{^{1}H} NMR (75 MHz, [D_6]benzene): $\delta = 139.2$ (d, ^1J(C,Rh) = 42 Hz, C_{ipso}), 133.2 (m, C_o), 127.9–128.1 ppm (m, $C_m + C_p$, PPh_3); ^{15}N–^{1}H HMQC (40 MHz, [D_6]benzene): $\delta = -5.6$ ppm; MS (ESI$^+$): *m/z*: 643.5 [M^+/2]; elemental analysis calcd (%) for $C_{72}H_{64}N_2P_4Rh_2$: C 67.19, H 5.01, N 2.18; found: C 67.01, H 4.89, N 2.09.

Synthesis of [{Rh(μ-NH_2)($PMePh_2$)$_2$}$_2$] (12): To a suspension of complex **1** (0.08 g, 0.17 mmol) in hexane (7 mL), pure methyldiphenylphosphane (0.22 g, 199 μL, 1.06 mmol) was slowly added through a syringe, giving rise to an orange solution, which was stirred for 40 min. Concentration of the volume by reduced pressure to dryness afforded an orange solid. This was washed repeatedly with hexane and then dried under vacuum (0.12 g, 65%). ^{1}H NMR (300 MHz, [D_6]benzene): $\delta = 7.96$ (m, 16H; H_o), 7.13 (m, 24H; $H_m + H_p$, PPh_2), 1.49 (m, 3H; PMe), −0.69 ppm (brs, 4H; NH_2); ^{31}P{^{1}H} NMR (121 MHz, [D_6]benzene): $\delta = 30.2$ ppm (d, ^1J(P,Rh) = 165 Hz); ^{13}C{^{1}H} NMR (75 MHz, [D_6]benzene): $\delta = 141.2$ (d, ^1J(C,Rh) = 35 Hz), 140.1 (d, ^1J(C,Rh) = 37 Hz), 139.8 (d, ^1J(C,Rh) = 34 Hz, C_{ipso}), 133.0 (m, $C_o + C_m$), 131.0 (d, ^3J(C,Rh) = 3 Hz, C_m), 130.6 (d, ^2J(C,Rh) = 9 Hz, C_o), 128.3 (d, ^2J(C,Rh) = 12 Hz, C_o), 127.3–127.9 (m, $C_m + C_p$, PPh_2), 17.8 (d, ^2J(C,P) = 13 Hz), 17.5 ppm (d, ^2J(C,P) = 13 Hz, PMe); ^{15}N–^{1}H HMQC (40 MHz, [D_6]benzene): $\delta = -9.6$ (brs, NH_2); MS (ESI$^+$): *m/z*: 518.9 [M^+/2].

Synthesis of [{Rh(μ-NH_2)(PMe_2Ph)$_2$}$_2$] (13): Pure dimethylphenylphosphane (0.23 g, 235 μL, 1.65 mmol) was slowly added through a syringe to a solution of complex **1** (0.12 g, 0.27 mmol) in toluene (3 mL), giving rise to an orange solution, which was stirred for 30 min. Concentration of the volume by reduced pressure to dryness afforded an orange solid. This was washed repeatedly with hexane and then dried under vacuum (0.18 g, 83%). ^{1}H NMR (300 MHz, [D_6]benzene): $\delta = 8.28$ (m, 8H; H_o), 7.31–7.20 (m, 12H; $H_m + H_p$, PPh), 1.15 (m, 24H; PMe_2), −0.30 ppm (brs, 4H; NH_2); ^{31}P{^{1}H} NMR (121 MHz, [D_6]benzene): $\delta = 12.1$ ppm (d, ^1J(P,Rh) = 166 Hz); ^{13}C{^{1}H} NMR (75 MHz, [D_6]benzene): $\delta = 144.0$ (m, C_{ipso}), 132.3 (m, C_o), 127.6–128.4 (m, $C_m + C_p$, PPh), 19.1 ppm (m, PMe_2); ^{15}N–^{1}H HMQC (40 MHz, [D_6]benzene): $\delta = -17.8$ (brs, NH_2); MS (ESI+): *m/z*: 395.0 [M^+/2]; elemental analysis calcd (%) for $C_{32}H_{48}N_2P_4Rh_2$: C 48.62, H 6.12, N 3.54; found: C 48.11, H 6.02, N 3.23.

Synthesis of [Ir(cod)(NH_2)($PMePh_2$)$_2$] (14): Pure methyldiphenylphosphane (28 mg, 26 μL, 0.14 mmol) was slowly added through a syringe to a solution of complex **2** (15 mg g, 0.023 mmol) in [D_8]toluene (0.5 mL), giving rise to a red solution. At this point, the conversion to complex **14** was found to be quantitative. ^{1}H NMR (300 MHz, [D_6]benzene): $\delta = 7.41$ (m, 8H; H_o), 7.05 (m, 12H; $H_m + H_p$, PPh_2), 3.14 (m, 4H; =CH), 2.01 (m, 4H; CH_2), 1.90 (m, 4H; CH_2 COD), 1.54 (m, 6H; CH_3P), −0.83 ppm (s, 2H, NH_2); ^{1}H NMR (300 MHz, [D_8]toluene, −40 °C): $\delta = 7.35$ (m, 6H; H_o), 7.08 (m, 12H; $H_m + H_p$, PPh_2), 3.81 (m, 2H), 2.85 (m, 2H; =CH COD), 1.91 (m, 2H), 1.76 (m, 2H; CH_2 COD), 1.37 (m, 6H; CH_3P), −1.34 ppm (s, 2H, NH_2); ^{31}P{^{1}H} NMR (162 MHz, [D_8]toluene): $\delta =$ −25.5 ppm (brs); ^{13}C{^{1}H} NMR (100 MHz, [D_8]toluene, −40 °C): $\delta =$ 140.7 (d, ^1J(C,P) = 13 Hz, C_{ipso}), 132.3 (d, ^2J(C,P) = 18 Hz, C_o), 128.5 (s, C_m), 128.3 (s, C_p, PPh_2), 66.7 (s, =CH), 58.5 (m, =CH), 34.5 (s, CH_2), 32.5 (s, CH_2 COD), 12.3 (d, ^1J(C,P) = 13 Hz, CH_3P); MS (ESI+): *m/z*: 717.1997 [M^+].

Synthesis of [Ir(cod)(OH)($PMePh_2$)$_2$] (15): A solution of complex **14** (0.02 g, 0.03 mmol) in THF (2 mL) was treated with water (0.02 g, 1.5 μL, 0.08 mmol) through a microsyringe. The resulting yellowish solution was stirred for 10 min at room temperature and then the volatiles were removed under vacuum, affording a light brown solid (0.02 g, 99%). ^{1}H NMR (400 MHz, [D_8]toluene, −40 °C): $\delta = 7.91$ (m, 6H; H_o), 7.48 (m, 2H; H_o), 7.42–7.28 (m, 12H; $H_m + H_p$, PPh_2), 3.31 (m, 2H), 3.20 (m, 2H; =CH COD), 2.27 (m, 2H; CH_2 COD), 2.13 (m, 10H; CH_2 COD + CH_3P), 1.97 (m, 2H; CH_2 COD), −2.71 ppm (s, 1H, OH); ^{31}P{^{1}H} NMR (162 MHz, [D_8]toluene, −40 °C): $\delta = -17.8$ ppm (s); ^{13}C{^{1}H} NMR (100 MHz, [D_8]toluene, −40 °C): $\delta = 142.1$ (d, ^1J(C,P) = 23 Hz), 141.9 (d, ^1J(C,P) = 23 Hz), 138.2 (d, ^1J(C,P) = 14 Hz), 138.1 (d, ^1J(C,P) = 15 Hz, C_{ipso}), 133.4 (m), 132.0 (m, C_o), 131.2 (d, ^3J(C,P) = 3 Hz, C_m), 130.8 (d, ^2J-(C,P) = 10 Hz, C_o), 129.3–128.0 (m, $C_m + C_p$, PPh_2), 61.0 (s, =CH), 58.5 (m, =CH), 35.1 (s, CH_2), 31.5 (s, CH_2 COD), 11.7 (d, ^1J(C,P) = 12 Hz), 11.5 ppm (d, ^1J(C,P) = 12 Hz, CH_3P).

Synthesis of [Ir(cod)(IPr)(NH_2)] (16): An NMR tube was charged with complex **2** (20 mg, 0.03 mmol), IPr (23 mg, 0.06 mmol), and carefully dried [D_6]benzene (0.4 mL), giving rise to a yellow solution within a minute. At this point, the formation of the novel complex **16** was almost quantitative. ^{1}H NMR (300 MHz, [D_6]benzene): $\delta = 7.41$ (m, 8H; H_o), 7.05 (m, 12H; $H_m + H_p$, PPh_2), 3.14 (m, 4H; =CH), 2.01 (m, 4H; CH_2), 1.90 (m, 4H; CH_2 COD), 1.54 (m, 6H; CH_3P), −0.83 ppm (s, 2H, NH_2); ^{1}H NMR (300 MHz, [D_8]toluene, −40 °C): $\delta = 7.29$–6.98 (m, 6H; Ph IPr), 6.42 (s, 2H; =CH IPr), 3.91 (m, 2H; =CH COD), 2.92 (m, 4H; CH *i*Pr), 2.55 (m, 2H; =CH), 2.00 (m, 4H; CH_2), 1.55 (m, 4H; CH_2 COD), 1.40 (d, ^3J(H,H) = 6.6 Hz, 12H; CH_3 *i*Pr), 1.00 ppm (d, ^3J (H,H) = 6.9 Hz, 12H; CH_3 *i*Pr); ^{13}C{^{1}H} NMR (75 MHz, [D_6]benzene): $\delta = 185.7$ (s, C-Ir IPr), 75.9, 46.6 (s, =CH), 34.9, 29.6 (s, CH_2 COD), 28.5 (s, CH), 26.2, 24.5 (s, Me *i*Pr); MS (ESI+): *m/z*: 717.1997 [M^+].

Synthesis of [Ir(cod)(IPr)(OH)] (17): A solution of complex **2** (0.07 g, 0.11 mmol) in toluene (5 mL) was treated with IPr (0.09 g, 0.23 mmol) giving a yellow solution, and then with water (7 μL, 0.46 mmol), and the resulting yellow mixture was stirred for 45 min. The volatiles were removed in vacuum, and the addition of hexane (8 mL) afforded a yellow solid, which was collected by filtration, washed with hexane, and then dried in vacuum (0.15 g, 95%). ^{1}H NMR (300 MHz, [D_6]benzene): $\delta =$ 7.29 (m, 2H; H_p), 7.25 (m, 4H; H_m, Ph IPr), 6.46 (s, 2H; =CH IPr), 3.78 (m, 2H; =CH COD), 2.90 (m, 4H; CH *i*Pr), 2.71 (m, 2H; =CH), 1.94 (m, 4H; CH_2), 1.45 (m, 2H; CH_2 COD), 1.42 (d, ^3J(H,H) = 6.6 Hz, 12H; CH_3 *i*Pr), 1.35 (m, 2H; CH_2 COD), 1.01 ppm (d, ^3J (H,H) = 6.9 Hz, 12H; CH_3 *i*Pr); ^{13}C{^{1}H} NMR (75 MHz, [D_6]benzene): $\delta = 186.3$ (s, C-Ir), 146.6 (s, C_q), 136.7 (s, C_q-N), 129.6 (s, $C_m + C_p$), 123.5 (s, =CHN IPr, 79.2, 45.5 (s, =CH), 34.5, 29.2 (s, CH_2 COD), 28.8 (s, CH), 26.1, 22.8 ppm (s, Me *i*Pr); MS (micro-TOF): *m/z*: 689.3487 [M^+−OH].

General protocol for the catalytic transfer hydrogenation: In a Schlenk tube, the catalyst (0.03 mmol), acetophenone (3 mmol), and an internal

standard (mesitylene, 250 μL) and, when needed Cs_2CO_3 (0.09 mmol), were dissolved in 2-propanol (3 mL). The reactor was then placed in a thermostated oil bath at 80 °C with vigorous stirring. Conversions were determined by gas chromatography techniques under the following conditions: column temperature: 40 °C (2 min) to 80 at 5 °C min^{-1} at a flow rate of 1 mL min^{-1} by using ultrapure He as carrier gas. The reaction progress was monitored by GC analysis in order to calculate the time dependence of the transfer hydrogenations of acetophenone. Aliquotes of 50 μL were taken in dichloromethane (1 mL) every 5 min for the first 30 min, every 10 min for the next 90 min, every 30 min for the next hour, and finally another two samples were taken after 360 min and a final one after 24 h from the beginning of the reaction. The samples were filtered through a syringe filter.

Crystal structure determination for complexes 2, 4, 5, and 7: X-ray diffraction data were collected at 100(2) K on a Bruker SMART APEX CCD (complexes **2** and **7**) and on a Bruker APEX II (complexes **4** and **5**) area detector diffractometers with graphite-monochromated $Mo_{K\alpha}$ radiation ($\lambda = 0.71073$ Å) by using narrow ω rotations (0.3°). Intensities were integrated and corrected for absorption effects with SMART,[42] SAINT+,[43] and SABABS[44] programs, included in APEX 2 package. The structures were solved by direct methods with SHELXS-97,[45] and refined by full-matrix least squares on F^2 with SHELXL-97.[46] Hydrogen atoms of the NH_2 bridges have been observed in Fourier difference maps and refined with a restraint in N–H distances. Particular details concerning the presence of solvent or static disorder are listed below.

Crystal data for complex 2: $3(C_{16}H_{28}Ir_2N_2)\cdot 1.5(C_6H_6)$; $M = 2015.57$; orange prism; $0.22\times0.19\times0.13$ mm^3; triclinic; $P\bar{1}$; $a = 9.2115(5)$, $b = 16.5730(8)$, $c = 19.9382(10)$ Å; $\alpha = 106.3240(10)$, $\beta = 90.6680(10)$, $\gamma = 104.2700(10)$°; $Z = 2$; $V = 2820.2(2)$ Å^3; $\rho_{calcd} = 2.374$ g cm^{-3}; $\mu = 14.139$ mm^{-1}, min. and max. transmission factors: 0.115 and 0.196; $2\theta_{max} = 56.96$°; 18548 reflections collected, 12330 unique [$R_{int} = 0.0178$]; number of data/restraints/parameters: 12330/12/659; final GoF: 1.051, $R_1 = 0.0281$ [10842 reflections, $I > 2\sigma(I)$], $wR2 = 0.0691$ for all data; largest difference peak: 1.694 e Å^3.

Crystal data for complex 4: $C_4H_4Ir_2N_2O_4$; $M = 528.49$; yellow needle; $0.34\times0.12\times0.07$ mm^3; monoclinic; $C2/c$; $a = 17.8094(12)$, $b = 4.0305(3)$, $c = 14.1144(10)$ Å; $\beta = 121.1610(10)$°; $Z = 4$; $V = 866.94(11)$ Å^3; $\rho_{calcd} = 4.049$ g cm^{-3}; $\mu = 30.644$ mm^{-1}, min. and max. transmission factors: 0.015 and 0.057; $2\theta_{max} = 58.5$°; 5063 reflections collected, 1126 unique [$R_{int} = 0.0311$]; number of data/restraints/parameters: 1126/1/63; final GoF: 1.118, $R_1 = 0.0227$ [1073 reflections, $I > 2\sigma(I)$], $wR2 = 0.0594$ for all data; largest difference peak: 2.915 e Å^3.

Crystal data for complex 5: $C_{17}H_{30}Cl_2Ir_2N_2$; $M = 717.73$; red prism; $0.08\times0.05\times0.02$ mm^3; monoclinic; $C2/c$; $a = 36.861(3)$, $b = 9.6577(7)$, $c = 10.4390(7)$ Å; $\beta = 90.0340(10)$°; $Z = 8$; $V = 3716.2(4)$ Å^3; $\rho_{calcd} = 2.558$ g cm^{-3}; $\mu = 14.597$ mm^{-1}, min. and max. transmission factors: 0.465 and 0.604; $2\theta_{max} = 60.02$°; 13405 reflections collected, 5107 unique [$R_{int} = 0.0369$]; number of data/restraints/parameters: 5107/4/249; final GoF: 0.999, $R_1 = 0.0323$ [4035 reflections, $I > 2\sigma(I)$], $wR2 = 0.0651$ for all data; largest difference peak: 2.271 e Å^3. Methylene chloride and chlorine atoms bounded to the metals have been found disordered. They have been included in the model in two sets of positions with complementary occupancy factors (0.66/0.34). Hydrogen atoms of the amido groups have been refined with a common isotropic thermal parameter. The highest residual density peak has been found close to an iridium atom. It has no chemical sense.

Crystal data for complex 7: $C_{16}H_{28}Cl_2Ir_2N_2\cdot C_7H_8$; $M = 795.84$; dark red pyramidal; $0.18\times0.16\times0.15$ mm^3; triclinic; $P\bar{1}$; $a = 11.0294(5)$, $b = 13.8433(7)$, $c = 16.0792(8)$ Å; $\alpha = 81.6060(10)$, $\beta = 84.1630(10)$, $\gamma = 77.1340(10)$°; $Z = 4$; $V = 2361.6(2)$ Å^3; $\rho_{calcd} = 2.238$ g cm^{-3}; $\mu = 11.497$ mm^{-1}, min. and max. transmission factors: 0.188 and 0.283; $2\theta_{max} = 57.42$°; 29063 reflections collected, 11077 unique [$R_{int} = 0.0235$]; number of data/restraints/parameters: 11077/9/591; final GoF: 1.062, $R_1 = 0.0225$ [9922 reflections, $I > 2\sigma(I)$], $wR2 = 0.0536$ for all data; largest difference peak: 1.217 e Å^3. The asymmetric unit contains two Ir atoms and two solvent toluene molecules. One of the latter has been found to be disordered; it has been modeled in two sets of positions with complementary occupancy factors. Hydrogen atoms of the amido groups have been refined with a common isotropic thermal parameter.

CCDC-913028 (**2**), CCDC-913029 (**4**), CCDC- (**5**), CCDC-913031 (**7**), and CCDC-913032 contain the supplementary crystallographic data for this paper. These data can be obtained free of charge from The Cambridge Crystallographic Data Centre via www.ccdc.cam.ac.uk/data_request/cif.

Acknowledgements

Financial support from CONSOLIDER INGENIO-2010 program under the projects MULTICAT (CSD2009-00050) and Factoría de Cristalización (CSD2006-0015) and project CTQ2012-35665 is acknowledged. P.G.O. acknowledges the CSIC "JAE-Doc" program, cofounded by the ESF and Factoría de Cristalización projects, for financial support. The authors express their appreciation to the support from the Ministry of Higher Education, Saudi Arabia, in establishment of the Center of Research Excellence in Petroleum Refining & Petrochemicals at King Fahd University of Petroleum & Minerals (KFUPM). The support of KFUPM is also highly appreciated.

[1] a) J. R. Fulton, A. W. Holland, D. J. Fox, R. G. Bergman, *Acc. Chem. Res.* **2002**, *35*, 44–56; b) H. E. Bryndza, W. Tam, *Chem. Rev.* **1988**, *88*, 1163–1188.

[2] a) T. E. Müller, K. C. Hultzsch, M. Yus, F. Foubelo, M. Tada, *Chem. Rev.* **2008**, *108*, 3795–3892; b) P. W. Roesky, T. E. Müller, *Angew. Chem.* **2003**, *115*, 2812–2814; *Angew. Chem. Int. Ed.* **2003**, *42*, 2708–2710; c) M. Nobis, B. Drießen-Hölscher, *Angew. Chem.* **2001**, *113*, 4105–4108; *Angew. Chem. Int. Ed.* **2001**, *40*, 3983–3985.

[3] a) J. F. Hartwig, *Nature* **2008**, *455*, 314–322; b) J. P. Wolfe, S. Wagaw, J. F. Marcoux, S. L. Buchwald, *Acc. Chem. Res.* **1998**, *31*, 805–818.

[4] a) T. Zweifel, J. V. Naubron, T. Büttner, T. Ott, H. Grützmacher, *Angew. Chem.* **2008**, *120*, 3289–3293; *Angew. Chem. Int. Ed.* **2008**, *47*, 3245–3249; b) M. Yamakawa, H. Ito, R. Noyori, *J. Am. Chem. Soc.* **2000**, *122*, 1466–1478; c) R. Noyori, M. Yamakawa, *Acc. Chem. Res.* **1997**, *30*, 97–102.

[5] J. Choi, A. H. R. MacArthur, M. Brookhart, A. S. Goldman, *Chem. Rev.* **2011**, *111*, 1761–1779.

[6] a) R. J. Lundgren, A, Sappong-Kumankumah, M. Stradiotto, *Chem. Eur. J.* **2010**, *16*, 1983–1991; b) T. Schulz, C. Torborg, S. Enthaler, B. Schaffner, A. Dumrath, A. Spannenberg, H. Neumann, A. Borner, M. Beller, *Chem. Eur. J.* **2009**, *15*, 4528–4533; c) G. D. Vo, J. F. Hartwig, *J. Am. Chem. Soc.* **2009**, *131*, 11049–11061; d) D. S. Surry, S. L. Buchwald, *J. Am. Chem. Soc.* **2007**, *129*, 10354–10355.

[7] a) H. H. Rao, H. Fu, Y. Y. Jiang, Y. F. Zhao, *Angew. Chem.* **2009**, *121*, 1134–1136; *Angew. Chem. Int. Ed.* **2009**, *48*, 1114–1116; b) C. F. Zhou, F. Chen, D. P. Yang, X. F. Jia, L. X. Zhang, J. Cheng, *Chem. Lett.* **2009**, *38*, 708–709.

[8] Q. Shen, J. F. Hartwig, *J. Am. Chem. Soc.* **2006**, *128*, 10028–10029.

[9] a) J. I. van der Vlugt, *Chem. Soc. Rev.* **2010**, *39*, 2302–2322; b) P. Brandi-Blanco, P. J. Sanz Miguel, B. Lippert, *Dalton Trans.* **2011**, *40*, 10316–10318; c) A. Singh; U. Anandhi, M. A. Cinellu, P. R. Sharp, *Dalton Trans.* **2008**, 2314–2327; U. Anandhi, M. A. Cinellu, P. R. Sharp, *Dalton Trans.* **2008**, 2314–2327; d) S. Kannan, A. J. James, P. R. Sharp, *Inorg. Chim. Acta* **2003**, *345*, 8–14; e) A. Schneider, E. Freisinger, B. Beck, B. Lippert, *J. Chem. Soc. Dalton Trans.* **2000**, 837–838; f) U. Anandhi, T. Holbert, D. Lueng, P. R. Sharp, *Inorg. Chem.* **2003**, *42*, 1282–1295; g) C. Q. Ye, P. R. Sharp, *Inorg. Chem.* **1995**, *34*, 55–59; h) Y. W. Ge, Y. Ye, P. R. Sharp, *J. Am. Chem. Soc.* **1994**, *116*, 8384–8385.

[10] a) J. Cámpora, P. Palma, D. del Río, M. M. Conejo, E. Álvarez, *Organometallics* **2004**, *23*, 5653–5655; b) D. J. Fox, R. G. Bergman, *J. Am. Chem. Soc.* **2003**, *125*, 8984–8985; c) A. W. Kaplan, J. C. M. Ritter, R. G. Bergman, *J. Am. Chem. Soc.* **1998**, *120*, 6828–6829.

[11] a) D. Conner, K. N. Jayaprakash, T. R. Cundari, T. B. Gunnoe, *Organometallics* **2004**, *23*, 2724–2733; b) M. Kanzelberger, X. Zhang,

T. J. Emge, A. S. Goldman, J. Zhao, C. Incarvito, J. F. Hartwig, *J. Am. Chem. Soc.* **2003**, *125*, 13644–13645.
[12] a) A. W. Holland, R. G. Bergman, *J. Am. Chem. Soc.* **2002**, *124*, 14684–14695; b) K. N. Jayaprakash, D. Conner, T. B. Gunnoe, *Organometallics* **2001**, *20*, 5254–5256; c) F. L. Joslin, M. P. Johnson, J. T. Mague, D. M. Roundhill, *Organometallics* **1991**, *10*, 2781–2794.
[13] T. Kimura, H. Arita, K. Ishiwata, S. Kuwata, T. Ikariya, *Dalton Trans.* **2009**, 2912–2914.
[14] J. Schöffel, A. Yu. Rogachev, S. D. George, P. Burguer, *Angew. Chem.* **2009**, *121*, 4828–4832; *Angew. Chem. Int. Ed.* **2009**, *48*, 4734–4738.
[15] T. Braun, *Angew. Chem.* **2005**, *117*, 5138–5140; *Angew. Chem. Int. Ed.* **2005**, *44*, 5012–5014.
[16] a) A. L. Casalnuovo, J. C. Calabrese, D. Milstein, *Inorg. Chem.* **1987**, *26*, 971–973; b) R. Koelliker, D. Milstein, *Angew. Chem.* **1991**, *103*, 724–726; *Angew. Chem. Int. Ed. Engl.* **1991**, *30*, 707–709; c) M. Schulz, D. Milstein, *J. Chem. Soc. Chem. Commun.* **1993**, 318–319; d) P. Kläring, S. Pahl, T. Braun, A. Penner, *Dalton Trans.* **2011**, *40*, 6785–6791; e) E. Morgan, D. F. MacLean, R. McDonald, L. Turculet, *J. Am. Chem. Soc.* **2009**, *131*, 14234–14236; f) M. A. Salomon, A. K. Jungton, T. Braun, *Dalton Trans.* **2009**, 7669–7677; g) C. M. Fafard, D. Adhikari, B. M. Foxman, D. J. Mindiola, O. V. Ozerov, *J. Am. Chem. Soc.* **2007**, *129*, 10318–10319.
[17] J. Zhao, A. S. Goldman, J. F. Hartwig, *Science* **2005**, *307*, 1080–1082.
[18] T. Kimura, N. Koiso, K. Ishiwata, S. Kuwata, T. Ikariya, *J. Am. Chem. Soc.* **2011**, *133*, 8880–8883.
[19] E. Khaskin, M. A. Iron, L. J. W. Shimon, J. Zhang, D. Milstein, *J. Am. Chem. Soc.* **2010**, *132*, 8542–8543.
[20] I. Mena, M. A. Casado, P. García-Orduña, V. Polo, F. J. Lahoz, L. A. Oro, *Angew. Chem.* **2011**, *123*, 11939–11942; *Angew. Chem. Int. Ed.* **2011**, *50*, 11735–11738.
[21] a) D. J. Fox, R. G. Bergman, *Organometallics* **2004**, *23*, 1656–1670; b) D. Conner, K. N. Jayaprakash, M. B. Wells, S. Manzer, T. B. Gunnoe, P. D. Boyle, *Inorg. Chem.* **2003**, *42*, 4759–4772; c) J. R. Fulton, S. Sklenak, M. W. Bouwkamp, R. G. Bergman, *J. Am. Chem. Soc.* **2002**, *124*, 4722–4737; e) J. R. Fulton, M. W. Bouwkamp, R. G. Bergman, *J. Am. Chem. Soc.* **2000**, *122*, 8799–8800.
[22] H. Roesky, S. Singh, K. K. M. Yusuff, J. A. Maguire, N. S. Hosmane, *Chem. Rev.* **2006**, *106*, 3813–3843.
[23] M. Albrecht, J. R. Miecznikowski, A. Samuel, J. W. Faller, R. H. Crabtree, *Organometallics* **2002**, *21*, 3596–3604.
[24] P. Kläring, S. Pahl, T. Braun, A. Pennera, *Dalton Trans.* **2010**, 6785–6791.
[25] I. Mena, M. A. Casado, V. Polo, P. García-Orduña, F. J. Lahoz, L. A. Oro, *Angew. Chem. Int. Ed.* **2012**, *51*, 8259–8263.
[26] I. Kownacki, B. Marciniec, M. Kubicki, *Chem. Commun.* **2003**, 76–77.
[27] Cambridge Structural Database, CCDC 2012. F. H. Allen, *Acta Crystallogr. Sect. B* **2002**, *58*, 380–388.
[28] P. García-Orduña, I. Mena, M. A. Casado, F. J. Lahoz, *Acta Crystallogr. Sect. C* **2012**, *68*, m113–m116.
[29] M. K. Kolel-Veetil, M. Rahim, A. J. Edwards, A. L. Rheingold, K. J. Ahmed, *Inorg. Chem.* **1992**, *31*, 3877–3878.
[30] a) V. Miranda-Soto, J. J. Pérez-Torrente, L. A. Oro, F. J. Lahoz, M. L. Martín, M. Parra-Hake, D. B. Grotjahn, *Organometallics* **2006**, *25*, 4374–4390; b) M. A. F. Hernandez-Gruel, J. J. Pérez-Torrente, M. A. Ciriano, A. B. Rivas, F. J. Lahoz, T. Dobrinovitch, L. A. Oro, *Organometallics* **2003**, *22*, 1237–1249; c) M. A. Casado, J. J. Pérez-Torrente, M. A. Ciriano, A. J. Edwards, F. J. Lahoz, L. A. Oro, *Organometallics* **1999**, *18*, 5299–5310; d) E. Fernández, A. Ruiz, S. Castillón, C. Claver, J. F. Piniella, A. Álvarez-Larena, G. Germain, *J. Chem. Soc. Dalton Trans.* **1995**, 2137–2142; e) D. de Montauzon, P. Kalck, R. Poilblanc, *J. Organomet. Chem.* **1980**, *186*, 121–130.
[31] a) A. Vizi-Orosz, R. Ugo, R. Psaro, A. Sironi, M. Moret, C. Zucchi, F. Ghelfi, G. Pályi, *Inorg. Chem.* **1994**, *33*, 4600–4603; b) D. E. Chebi, P. E. Fanwick, I. P. Rothwell, *Polyhedron* **1990**, *9*, 969–974; c) L. A. Oro, M. J. Fernández, J. Modrego, J. M. López, *J. Organomet. Chem.* **1985**, *287*, 409–417.
[32] a) M. K. Kolel-Veetil, A. L. Rheingold, K. J. Ahmed, *Organometallics* **1993**, *12*, 3439–3446; b) M. J. Fernández, J. Modrego, L. A. Oro, M. C. Apreda, F. H. Cano, C. Foces-Foces, *Inorg. Chim. Acta* **1989**, *157*, 61–64; c) L. A. Oro, M. J. Fernández, J. Modrego, C. Foces-Foces, F. H. Cano, *Angew. Chem.* **1984**, *96*, 897–898; *Angew. Chem. Int. Ed. Engl.* **1984**, *23*, 913–914.
[33] M. A. Ciriano, A. R. Dias, P. M. Nunes, L. A. Oro, M. F. Minas da Piedade, M. E. Minas da Piedade, P. Ferreira da Silva, J. A. Matinho-Simoes, J. J. Pérez-Torrente, L. F. Veiros, *Struct. Chem.* **1996**, *7*, 337–354.
[34] M. T. Pinillos, A. Elduque, L. A. Oro, F. J. Lahoz, F. Bonati, A. Tiripicchio, M. Tiripicchio-Camellini, *J. Chem. Soc. Dalton Trans.* **1990**, 989–994.
[35] H. Werner, M. Müller, P. Steiner, *Z. Anorg. Allg. Chem.* **2003**, *629*, 1337–1346.
[36] a) C. Tejel, M. A. Ciriano, J. A. López, F. J. Lahoz, L. A. Oro, *Organometallics* **1998**, *17*, 1449–1451; b) C. Tejel, M. A. Ciriano, J. A. López, F. J. Lahoz, L. A. Oro, *Organometallics* **2000**, *19*, 4977–4984.
[37] M. A. Ciriano, J. J. Pérez-Torrente, L. A. Oro, *J. Organomet. Chem.* **1993**, *445*, 273–281.
[38] J. V. Caspar, H. B. Gray, *J. Am. Chem. Soc.* **1984**, *106*, 3029–3030.
[39] C. Tejel, M. A. Ciriano, M. Bordonaba, J. A. López, F. J. Lahoz, L. A. Oro, *Chem. Eur. J.* **2002**, *8*, 3128–3138.
[40] P. Zhao, C. Krug, J. F. Hartwig, *J. Am. Chem. Soc.* **2005**, *127*, 12066–12073.
[41] B. J. Truscott, G. C. Fortman, A. M. Z. Slawin, S. P. Nolan, *Org. Biomol. Chem.* **2011**, *9*, 7038–70412.
[42] SMART, 5.611, Bruker AXS, Inc., Madison, USA, **2000**.
[43] SAINT+, 6.01, Bruker AXS, Inc., Madison, USA, **2000**.
[44] G. M. Sheldrick, SADABS program University of Göttingen, Göttingen, Germany, **1999**,.
[45] G. M. Sheldrick, *Acta Crystallogr. Sect. A* **1990**, *46*, 467–473.
[46] G. M. Sheldrick, *Acta Crystallogr. Sect. A* **2008**, *64*, 112–122.

Received: December 10, 2012
Published online: March 15, 2013

